Available online at www.sciencedirect.com
ScienceDirect
Journal of Colloid and Interface Science 318 (2008) 322–330
JOURNAL OF Colloid and Interface Science
www.elsevier.com/locate/jcis

Water evaporation rates across hydrophobic acid monolayers at equilibrium spreading pressure

Minami Tsuji [a], Hiromichi Nakahara [a], Yoshikiyo Moroi [b], Osamu Shibata [a,b,*]

[a] *Division of Biointerfacial Science, Graduate School of Pharmaceutical Sciences, Kyushu University, 3-1-1 Maidashi, Higashi-ku, Fukuoka 812-8582, Japan*
[b] *Department of Biophysical Chemistry, Faculty of Pharmaceutical Sciences, Nagasaki International University, 2825-7 Huis Ten Bosch, Sasebo, Nagasaki 859-3298, Japan*

Received 3 September 2007; accepted 29 October 2007

Abstract

The effect of alkanoic acid [$CH_3(CH_2)_{n-2}COOH$; HCn] and perfluoroalkanoic acid [$CF_3(CF_2)_{n-2}COOH$; FCn] monolayers on the water evaporation rate was investigated by thermogravimetry tracing the decrease in amount of water with time. The evaporation rate from the surface covered by a monolayer was measured as a function of temperature and hydrophobic chain length of the acids, where the monolayer was under an equilibrium spreading pressure. From thermal behavior of the crystallized acids, their solid states are C-type in crystalline state over the temperature range from 298.2 to 323.2 K. The dry air was flowed through a furnace tube of a thermogravimetry apparatus at the flow rate of 80 mL min^{-1}, where the evaporation rate becomes almost constant irrespective of the flow rate. The temperature dependence of the evaporation rate was analyzed kinetically to evaluate the activation energy and thermodynamics values for the activated complex, which demonstrated that these values were almost the same for both alkanoic acids and perfluoroalkanoic acids, although the effect of perfluoroalkanoic acids on the evaporation rate was smaller than that of corresponding hydrogenated fatty acids. The difference in the evaporation rate between FCn and HCn was examined by atomic force microscopy (AFM), Brewster angle microscopy (BAM), surface potential (ΔV) at equilibrium spreading pressure, and Langmuir curve (π–A isotherm), and their results were consistent and supported the difference.

Keywords: Fluorinated amphiphiles; Perfluoroalkanoic acids; Evaporation rate of water; Thermogravimetry (TG); Differential scanning calorimetry (DSC); Equilibrium spreading pressure (ESP); Atomic force microscopy (AFM)

1. Introduction

Evaporation is a typical example of material transport across gas/liquid interface. The evaporation rate of water has been investigated since last about 80 years. Most of the investigations have used an indirect method to determine the amount of liquid evaporated; for example, the amount of evaporated water was measured by suspending a flat container with a permeable bottom supporting a solid desiccant (calcium chloride) over the surface of water in a film balance trough [1,2], where 100% water evaporated from the surface is not necessarily adsorbed into desiccant. A more reliable method would be indispensable for more quantitative analysis and for further understanding of the evaporation rate of water. Therefore, the method which directly measures the evaporation rate by tracing the weight loss of water with time was proposed [3,4]. The results thus obtained for several systems indicated that there was no difference in the evaporation rate and the activation energy among evaporations across an adsorbed layer of soluble surfactant and the one just from purified water, whereas insoluble monolayer decreased the evaporation rate and increased the activation energy [5–7]. An investigation on water evaporation across air/water interface just like the present study would be quite valuable from the view-point of water control all over the world against the forthcoming temperature increase of the earth.

Until now, the experiments of evaporation across a monolayer have been made mainly on hydrocarbon monolayer and little on fluorocarbon one. Fluorocarbons are now in wide-

* Corresponding author.
E-mail address: wosamu@niu.ac.jp (O. Shibata).
URL: http://www.niu.ac.jp/~pharm1/lab/physchem/indexenglish.html.

0021-9797/$ – see front matter
doi:10.1016/j.jcis.2007.10.047

spread use not only for scientific fields but also for practical purposes because of their hydrophobicity, lipophobicity, stability against acid and base, and thermal stability [8–12]. In particular, perfluoroalkanoic acids are most commonly employed to examine whether alkanoic acids can be replaced by perfluoroalkanoic acids due to their excellent physico-chemical properties and to see their new functions. Toxicokinetics of perfluoroalkanoic acids has also been investigated, where they seem to have a high potential for bioaccumulation [10,13]. In addition, such hazardous properties as skin and eye irritation, skin sensitization, and genotoxity were not identified as for hydrofluoropolyethers [14]. In practice, perfluoropolyethers are nowadays applied to cosmetics. The physico-chemical behavior of perfluoroalkanoic acid as Langmuir monolayer has been precisely investigated [15], but reports on the retardation effect of perfluoroalkanoic acid on water evaporation are quite few in number, as far as the authors know, although dynamic surface excesses of fluorocarbon had been investigated in the different way by Eastoe et al. [16].

This study aims to compare the effect of fluorocarbon monolayer on water evaporation with that of hydrocarbon monolayer and to examine which part of the molecules, hydrophobic chain or hydrophilic group, contributes to the depression of water evaporation. The evaporation is also examined by the theory of absolute reaction rate to see the difference between hydrocarbon and fluorocarbon from the thermodynamic point of view for the activated complex formation. The present basic study on water evaporation will certainly serve to further work on evaporation across air/liquid interface.

2. Experimental

2.1. Materials

Perfluorodecanoic acid (FC10), perfluorododecanoic acid (FC12), perfluorotetradecanoic acid (FC14), perfluorohexadecanoic acid (FC16), and perfluorooctadecanoic acid (FC18) were obtained from Fluorochem (United Kingdom). These acids were purified by recrystallization with *n*-hexane/acetone mixed solvents after distillation once, and their purity was checked by ^{19}F NMR spectra (UNITY INOVA 400 Spectrometer, Varian, USA) and by elemental analysis [17]. As for the elemental analysis, the observed and calculated values were in satisfactory agreement ($< \pm 0.3\%$ for carbon atom). Their purity was also confirmed to be more than 99.5% by GC-MS (QP-1000, Shimadzu, Kyoto). *n*-Hexane of analytical reagent grade, acetone of highest grade, and ethanol of especially prepared reagent were bought from nacalai tesque (Kyoto, Japan). They were used as a solvent for recrystallization above and as a spreading solvent for Langmuir isotherm measurements. Dodecanoic acid (HC12), tetradecanoic acid (HC14), hexadecanoic acid (HC16), and octadecanoic acid (HC18) were purchased from SIGMA (99–100%) and used without further purification. The substrate solutions of pH 1 and 2 were prepared using thrice-distilled water and concentrated H_2SO_4 (Wako Chemical Co.) or HCl (nacalai tesque, Kyoto). As for the whole acids crystallized from the molten state, any solid phase-transition was not observed over the temperature range from 298.2 to 323.2 K by DSC measurement [17]. The water used in the present study was thrice distilled (surface tension = 71.96 mN m^{-1} at 298.2 K, and electrical resistivity = 18 MΩ cm).

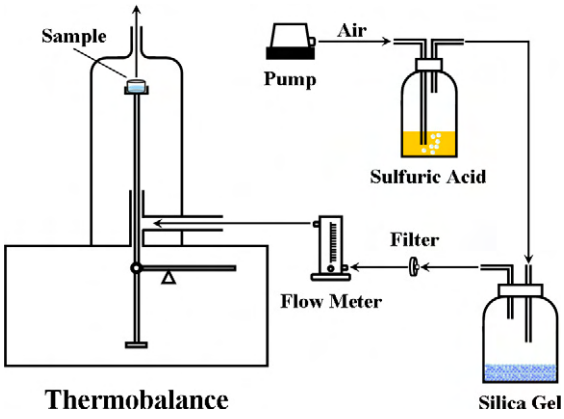

Fig. 1. Schematic illustration of the modified apparatus for thermogravimetry.

2.2. Evaporation rate

The apparatus used for evaporation rate was a modified thermobalance (Fig. 1, Rigaku Thermo Plus 2) as reported previously [4], where the sample pan had a large area (0.739 cm^2) to make an edge effect as small as possible. The apparatus can detect the changes of both weight and temperature with time simultaneously, where the temperature was controlled within ±0.1 K throughout a run except for initial fluctuation. The dry air flowing through a furnace tube at a constant temperature is able to reduce the stagnant gaseous layer formed just above the surface. Moisture in the flowing air from a small air pump was removed first by passing through concentrated sulfuric acid and second by being kept over dried silica gel. The flow rate was controlled by a flow meter with a needle bulb. The experimental reproducibility was confirmed by superimposing the traces of the weight decrease with time for the same sample, which means that the rate measurement is very accurate. A 150 μL of liquid sample (aqueous solution saturated by a hydrophobic acid) was pipetted into the platinum pan, and then, a tiny particle of the solid acid was placed on the surface of the solution, where a solid from the molten (molten solid) was used in order to unify a crystal structure. The initial depth of liquid was 0.20 cm at the center of pan and the height from the surface of liquid to the top of the pan was 0.48 cm. Such a thin layer of liquid is easy for the thermister just beneath the pan thermally to follow the liquid temperature. From dependence of the evaporation rate on the duration for spreading, the standing period of time was decided for each hydrophobic acid. For example, 24 h standing was needed for FC10 to reach the constant evaporation rate, which means that the monolayer on the water surface is in equilibrium with the solid. Then, the pan was set in a furnace tube for the gravitational measurement over the temperature range from 298.2 to 323.2 K. The run was started without allowing thermal equilibrium with the furnace temperature due to the small thermal mass of the sample. All the acids

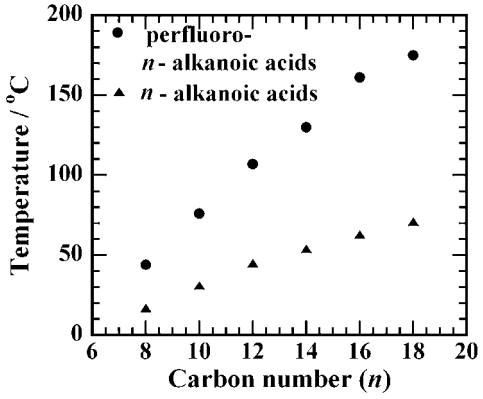

Fig. 2. Change in melting point of FC*n* and HC*n* against the number of carbon atoms of the acids.

used in the present study were examined below their melting point (Fig. 2).

2.3. ESP measurement

Surface pressure (π) change with time (t) for the acids was traced by the Wilhelmy plate method under atmospheric pressure at 298.2 K to determine respective equilibrium spreading pressure (ESP) and time to reach it. The pressure-measuring system (KSV Minitrough, KSV Instruments Ltd., Finland) was equipped with a filter paper (Whatman 541, periphery = 2 cm). Thrice-distilled water was used as a substrate solution. The experimental error was ± 0.1 mN m^{-1}.

2.4. Atomic force microscopy

Sample preparation of a monolayer was carried out by the horizontal lifting method. Graphite (SPI000E045, 5 × 5 mm, Seiko Instruments Inc.) was used as a supporting solid substrate for the monolayer deposition. A horizontal graphite substrate was made to descend until it comes to contact with the monolayer on the water subphase under equilibrium spreading pressures at 298.2 K. After contacting the monolayer, the graphite was lifted at the velocity of 1 mm min^{-1}. The LB films with deposition rate of ∼1 were used in the experiments. AFM images were obtained using a SPA 400 instrument (Seiko Instruments Inc.) at 298.2 ± 2 K in a tapping mode, which provided both a topographical image and a phase contrast one. The tapping mode images were collected at scan rates of 0.5–3 Hz, using silicon tips (Olympus Co., Tokyo, Japan) with a nominal spring constant of 1.8 N m^{-1} under the normal atmosphere.

3. Results and discussion

3.1. Evaporation rate by TG

The stagnant vapor layer above a liquid surface may influence the evaporation rate. Therefore, study was made first on the effect of the flow rate of dry air on the evaporation rate of water at three different temperatures, 303.2, 313.2, and 323.2 K. As a result, the effect of the flow rate was significant at lower

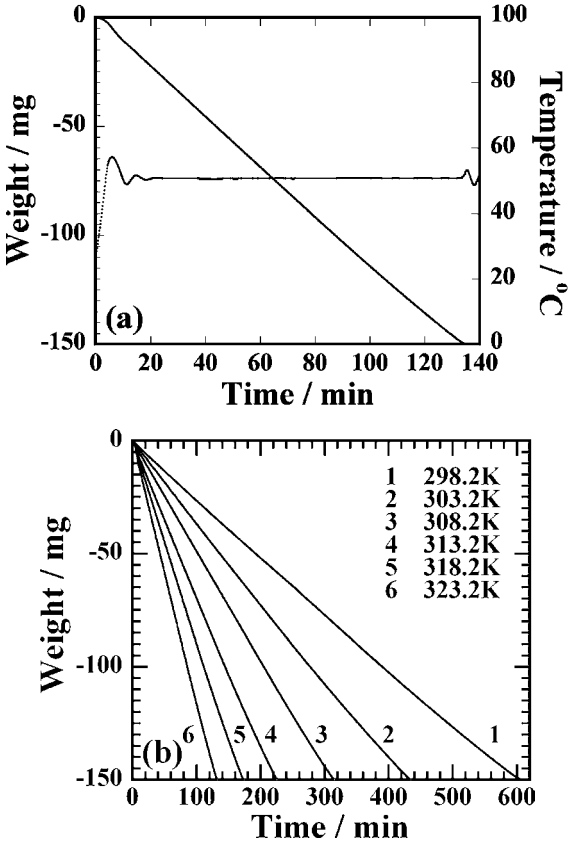

Fig. 3. Traces of weight change of water and temperature with time (a). Trace of the weight change at different temperatures from 298.2 to 323.2 K (b).

rate, whereas it became less significant at higher rate [3,6]. In all the present experiments, therefore, the flow rate was kept constant at 80 mL min^{-1} in order to minimize the effect of the flow rate drift, where the evaporation rate becomes almost constant irrespective of the flow rate.

First, weight decrease of water by vaporization from just liquid water surface, upon which there is no external resistance or no barrier against the water evaporation, was measured over the temperature range 298.2–323.2 K (Fig. 3). These data were used as a reference to investigate the effect of various monolayers on the evaporation rate of water. The evaporation rate (k) in units of mol s^{-1} cm^{-2} was calculated from the slope of weight decrease of water with time excluding the initial and the end parts of the relationship between the weight and time. As is clear from the traces of weight change, an excellent linearity is held at each temperature.

Next, weight decrease of water by evaporation from the surface covered by alkanoic acid monolayer was measured over the temperature range 298.2–323.2 K. Weight decrease of water by evaporation from the surface covered by FC14 and HC14 monolayers at different temperatures are illustrated in Figs. 4a and 4b, respectively, where it takes more than two hours for 150 μL water to evaporate. The results for other FC*n* and HC*n* are similarly obtained. A good linearity for weight loss vs time suggests that the FC*n* or HC*n* monolayer locates at the surface under the equilibrium state [5]. As for all acids examined here, the evaporation rate increased with increasing temperature. The

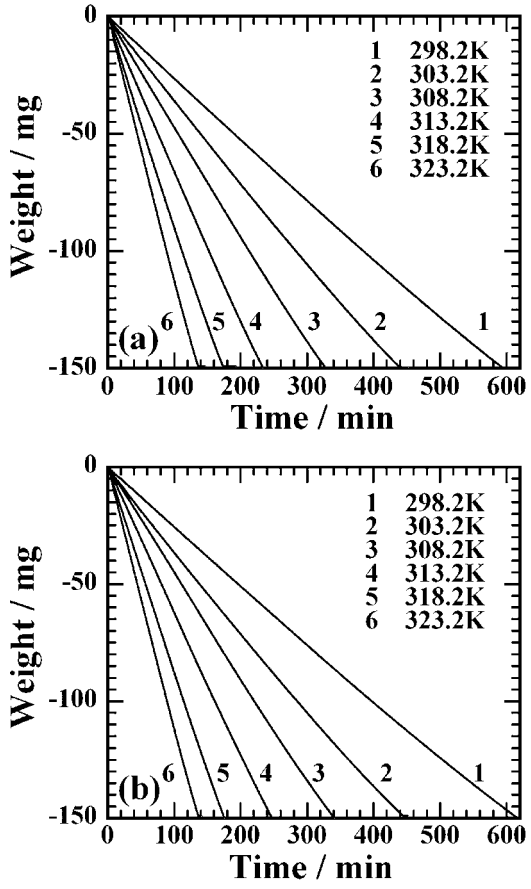

Fig. 4. Trace of the weight change with time due to water evaporation from surface covered by (a) FC14 or (b) HC14 monolayer at different temperatures from 298.2 to 323.2 K.

rate determination across the monolayer was made similarly as that just for water. Fig. 5 shows the evaporation rates for FC*n* and HC*n* at different temperatures. The results for HC*n* indicate that the evaporation rates increase with increasing temperature, whereas they decrease with increasing chain length. The effect of alkanoic acid monolayers (Fig. 5b) on the suppression of water evaporation increased in the order of HC12 < HC14 < HC16 < HC18. As for FC*n* in Fig. 5a, on the other hand, smaller suppression effect was observed at 313.2, 318.2, and 323.2 K, where the effect of the chain length was found to be quite small. In addition, the effect becomes less with increasing chain length, which is discussed later with surface potential of monolayer under equilibrium spreading pressure and with the relative decrease in evaporation rate [1,6,18].

It has already been shown that the effect of a monolayer or the retardation effect depends on chain length of HC*n*; that is, the retardation effect of alkanoic acid monolayer on water evaporation increased with increasing chain length. Barnes calculated the resistance to water evaporation, and then the resistance values were found to increase with increasing chain length [2,19]. Our present data for HC*n* agreed well with the previous ones.

The evaporation of water through 1-alkanol monolayer has already been investigated by a direct method as is the case of

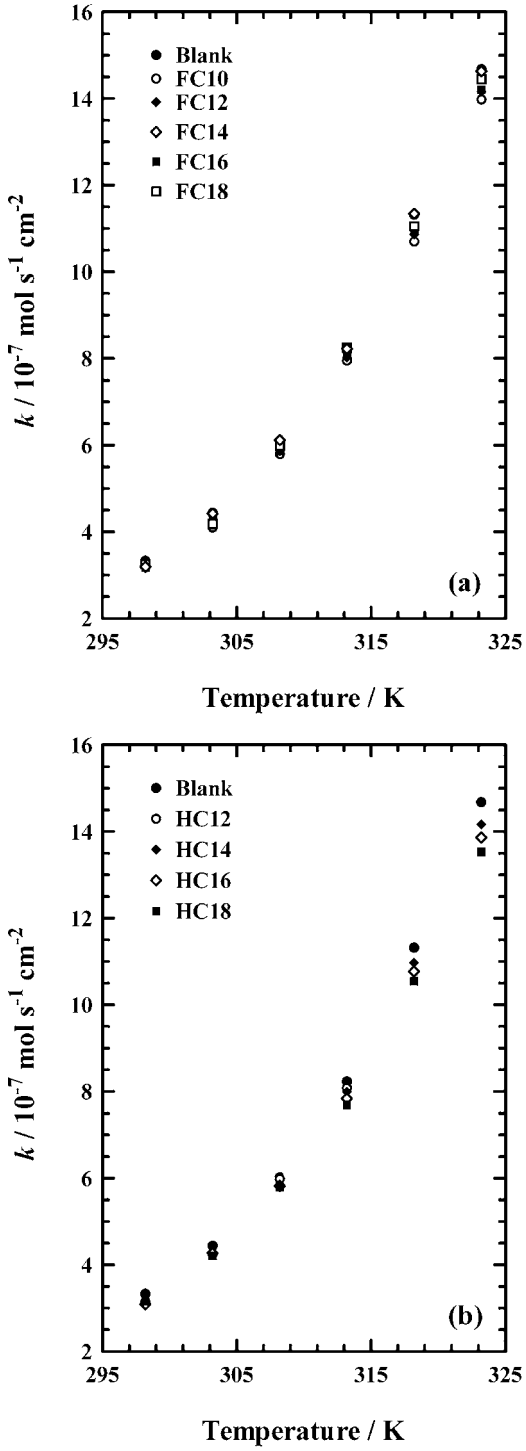

Fig. 5. Temperature dependence of evaporation rate of water from the surface covered by a monolayer of perfluoroalkanoic acids (a) and alkanoic acids (b) under the equilibrium spreading pressure.

the present paper [6]. The retardation effect of 1-alkanols on water evaporation increased with increasing the chain length just like HC*n*. However, the effect of the former was much larger than that of the present alkanoic acids (HC*n* and FC*n*). This difference may be due to stronger hydrophilicity of carboxyl group than hydroxyl group or to ionic dissociation of carboxylic group, which might bring about breakage of steric

Table 1
Evaporation rate of water (k) from the surface covered by HC14, FC12, FC16 monolayers at 323.2 K on water, 0.01 M HCl, and 0.1 M H_2SO_4 subphases

Materials	k (mol s^{-1} cm^{-2})		
	Water	0.01 M HCl (pH 2)	0.1 M H_2SO_4 (pH 1)
HC14	14.2	14.2	14.4
FC12	14.2		14.2
FC16	14.5		14.5

structure formed by water molecules [20] and the resultant easy escape of the molecules.

Difference in pK_a value between perfluoroalkanoic acids and alkanoic acids also supports that FCn has higher degree of dissociation [10,21,22] or stronger hydrophilicity than HCn. To investigate the influence of the degree of dissociation on the water evaporation, pH of subphase was changed. The evaporation rate from 0.01 M HCl (pH 2) and 0.1 M H_2SO_4 (pH 1) solutions was as same as that from purified water. Table 1 showed the evaporation rates of water (k) from the surface covered by HC14, FC12, FC16 monolayers at 323.2 K on just water, 0.01 M HCl, and 0.1 M H_2SO_4 subphases, and then those values showed no difference within the experimental error. Thus, there was no dependence in the evaporation rate on pH of the subphase. Therefore, the degree of dissociation could not apparently explain the difference in water evaporation rate. However, it is certain that the retardation effect on water evaporation rate decreased in the order of 1-alkanol > HCn > FCn. Thus, it might be highly possible that a hydroxyl group of alkanol can contribute much to the stabilization of the water structures than a carboxyl group. On the other hand, the acids, especially perfluoroalkanoic acid of larger dissociation degree, might easily break hydrogen bonds of water molecules due to its own resonance effect of the dissociated –COO^- group irrespective of bulk pH value. In addition, the smaller depression effect might be due to weaker intermolecular forces among FCn hydrophobic chains and between water molecule and fluorocarbon chain, where the less intermolecular interaction for FCn chain can be easily verified by smaller surface tension and lower boiling point of perfluorinated acids than those of hydrogenated ones. Then, it is certain that water molecules can move more easily though fluorocarbon chains than through hydrocarbon chains. That is, FCn molecules would form a monolayer to which water molecules are easy to permeable.

3.2. Theoretical analysis

Now that the smaller depression effect for FCn monolayer than for HCn one was made clear, it is quite important to quantify the extent of the depression, for which the relative decrease in evaporation rate is commonly employed. The rate of water evaporation is governed by the driving force for the evaporation and by the total permeation resistance through the transport pathway, whose equation is analogous to Ohm's law for electrical conductance [1,6,18],

$$J = \frac{\Delta C_g}{r_g} = \frac{\Delta C_t}{\sum_i r_i}, \tag{1}$$

where J is an evaporation flux at a stationary state, ΔC_g ($= C_{eq} - C_v$) is the difference between the water vapor concentrations driving the evaporation (C_{eq} is the concentration at a stationary evaporation rate just above the surface of water and C_v is the concentration in the atmosphere at some distance above the surface), r_g is a resistance in gas phase, and $\sum_i r_i$ is the total permeation or evaporation resistance, the sum of all the resistances that arise from sections of the pass way including the bulk water. ΔC_t is the total difference between water concentration in a bulk water and C_v. For evaporation of just water, the total resistance is denoted by $\sum r_w$, while for the evaporation from water surface covered by an insoluble monolayer of resistance r_m the total resistance becomes $\sum r_f$ (f refers to a film):

$$\sum r_f = \sum r_w + r_m. \tag{2}$$

The performance for a monolayer is often reported as the ratio, ϕ, of the evaporation rate with an insoluble monolayer to the rate just for liquid water ($\phi = J_f/J_w$) or as the relative decrease in evaporation rate (effectiveness of evaporation reduction) defined by $1 - \phi$, where the fluxes J_w and J_f refer to an evaporation rate of just liquid water and that from surface covered by insoluble monolayer, respectively. ΔC_t can be kept constant in the present experiment, and therefore, the relative decrease is express as

$$1 - \phi = \frac{r_m}{\sum r_w + r_m}. \tag{3}$$

The values of the relative decrease for the insoluble monolayers are summarized in Table 2 for the present study. Now it is quite clear that the depression effect is larger for HCn than for FCn, and the relative decrease is less than several percent. In addition, the decrease goes through a minimum with increasing temperature, which might result from the balance of kinetic motion between water molecules and insoluble molecules at the surface.

The activation energy of water evaporation from the surface covered by FCn or HCn monolayer can be calculated from the temperature dependence of the evaporation rate employing the following Arrhenius equation,

$$\ln k = A - E_a/RT, \tag{4}$$

where k is the evaporation rate per unit area (mol s^{-1} cm^{-2}), E_a is the activation energy (kJ mol^{-1}), T is the absolute temperature, R is the gas constant, and A is an arbitrary constant. The E_a value thus obtained includes the energy to break hydrogen bonds of water molecules and to overcome the resistance by the monolayer. The temperature dependence of the activation energy was calculated from the slope of the $\ln k$ vs T^{-1} plots at a given temperature. The evaporation process is endothermic and the E_a value vs total carbon number was illustrated in Fig. 6, where the E_a values are nearly equal to hydrogen-bond energy of water molecules. The activation energy slightly decreases with increasing temperature. When an FCn or an HCn monolayer is on the water surface, the evaporation rate (k) becomes smaller than that of blank water (no monolayer), whereas the activation energies of the evaporation through FCn or HCn

Table 2
The relative decrease in evaporation rate $(1-\phi)$

T (K)	$1-\phi$								
	FC10	FC12	FC14	FC16	FC18	HC12	HC14	HC16	HC18
298.2	0.036	0.018	0.048	0.024	0.042	0.054	0.066	0.072	0.054
303.2	0.077	0.056	0.014	0.059	0.005	0.043	0.041	0.038	0.052
308.2	0.037	0.025	0.027	0.005	−0.017	0.005	0.027	0.033	0.037
313.2	0.034	0.026	0.011	−0.001	0.001	0.018	0.029	0.047	0.066
318.2	0.055	0.041	0.031	0.024	−0.002	–	0.031	0.049	0.069
323.2	0.048	0.035	0.033	0.016	0.003	–	0.035	0.056	0.078

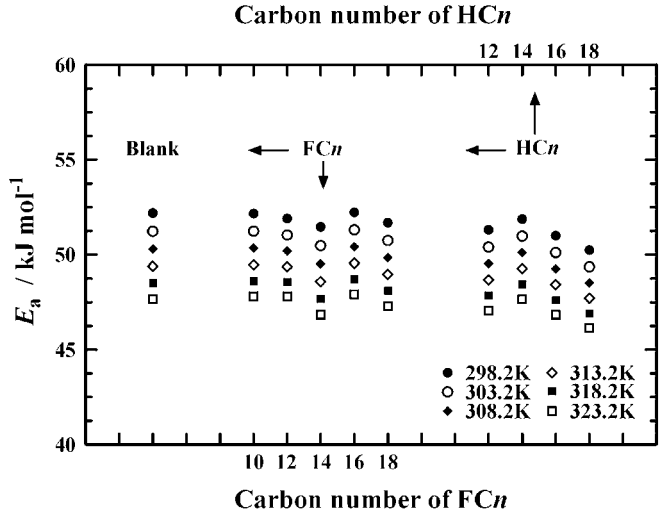

Fig. 6. The activation energy of water evaporation from the surface covered by the acid monolayers vs carbon number of the acids at different temperatures.

monolayer are nearly the same as that just from blank water. This fact strongly suggests that the difference in evaporation rate (k) is not reflected upon the activation energy which is closely connected with chemical reaction. The process of water evaporation includes breakage of strong hydrogen bonds of water molecules. That is, the E_a value mostly includes the energy to break the hydrogen bonds of water molecules or enthalpy change for the evaporation which decreases from 44.0 kJ mol^{-1} at 298.2 K down to 42.7 kJ mol^{-1} at 333.2 K [23]. Therefore, the presence of FCn or HCn monolayers might not be so effective as to influence chemical bond breakage.

On the other hand, the Gibbs energy change of activation ($\Delta^{\ddagger}G$) was also calculated using the Eyring equation [24],

$$k_2 = \kappa \frac{k_B T}{h} \overline{K} \tag{5}$$

and

$$\Delta^{\ddagger}G = -RT \ln \overline{K}, \tag{6}$$

where k_2 is the rate constant, k_B is the Boltzmann constant, T is absolute temperature, h is the Planck's constant, $\overline{K}$ is the equilibrium constant, R is the gas constant, and κ (transmission coefficient) is assumed to be unity. The k_2 value in the present study was evaluated by the evaporation rate; $k = k_2 C_w(T)$, where $C_w(T)$ is a molar concentration of bulk water at temperature T. In addition, the enthalpy change $\Delta^{\ddagger}H$ and the entropy change $\Delta^{\ddagger}S$ were calculated by Eq. (7),

$$\Delta^{\ddagger}G = \Delta^{\ddagger}H - T\Delta^{\ddagger}S, \tag{7}$$

where $\Delta^{\ddagger}H$ was evaluated by the temperature dependence of $\Delta^{\ddagger}G$. The values of $\Delta^{\ddagger}G$, $\Delta^{\ddagger}H$, and $\Delta^{\ddagger}S$ thus evaluated are shown in Figs. 7a, 7b, and 7c, respectively. The Gibbs energy changes of activation across the acid monolayer are nearly the same as that for just water, as is expected from E_a values in Fig. 6. The E_a values are nearly equal to the $\Delta^{\ddagger}H$ values which correspond to the magnitude of hydrogen bond energy. There is no explicit allowance for the difference of the evaporation rate between from just water and through FCn layer (Figs. 7b and 7c). The thermodynamic parameters were found not to explain the effects of hydrophobic chain or hydrophilic head group for FCn.

Table 3
Time of period for acids to reach the equilibrium spreading pressure

	n				
	10	12	14	16	18
FCn	<36 h	<50 h	<50 h	<50 h	<50 h
HCn		<2 h	<2 h	<36 h	<36 h

3.3. State of monomolecular films

The time to reach an equilibrium spreading pressure (t^{eq}) becomes longer with increasing chain length (Table 3). The standing time after placing FCn or HCn solid on water surface for the TG measurements was made longer than t^{eq}, which indicated that the monolayer used in this study was under equilibrium spreading pressure. Equilibrium spreading pressures (ESPs) of FCn and HCn are shown in Fig. 8. The ESP values for HCn decreased with increasing chain length. The same tendency was also seen in the reported values for HCn [25–28]. However, these values were found not to be closely related with the retardation effect on water evaporation. This fact clearly indicates that evaporation takes place just at the gas/liquid interface, whereas surface tension is integration of whole interaction energies among whole molecules in a bulk domain. What can be said from Fig. 8 is that FCn with higher dissociable –COOH group has stronger effect to reduce molecular interaction in surface layer.

In order to inquire further the monolayer state of the acids, the curves for surface pressure (π) against molecular area (A) were measured. Unfortunately, HCn ($n = 12, 14, 16$) and FCn ($n = 10, 12, 14$) are soluble in water, and therefore, a stable

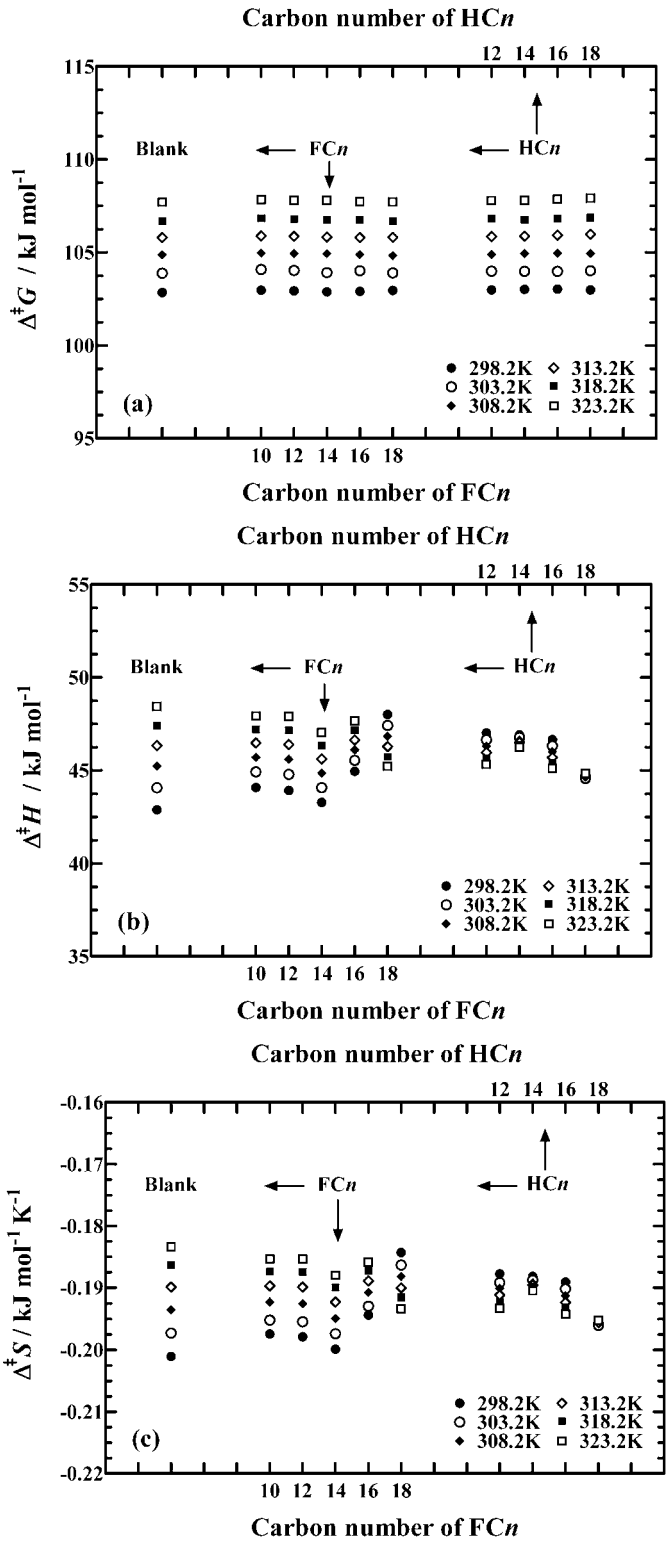

Fig. 7. Variations of the Gibbs energy change (a), enthalpy change (b), and entropy change (c) for the activation complex with carbon number of the acids.

π–A curves was not obtained for them. The π–A isotherms at 298.2 K for HC18, FC16, and FC18 are shown in supplementary Fig. S3. The ESP values for FCn (42 for FC16 and 36 mN m^{-1} for FC18) are above the corresponding collapse pressure (25 for FC16 and 30 mN m^{-1} for FC18) indicated by

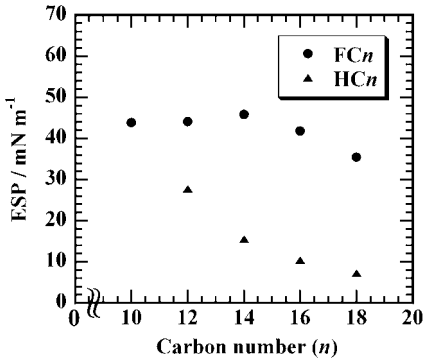

Fig. 8. Equilibrium spreading pressure (ESP) of perfluoroalkanoic acids (●) and alkanoic acids (▲) at 298.2 K.

arrows. These values of collapse pressures are almost the same as those reported previously [15]. Above the collapse pressure, the π–A isotherms did not become reproducible. Nonetheless, a solid state of FC16 and FC18 starts to appear on the surface at the collapse pressure, where a chemical potential of the acids becomes equal between the solid and the monolayer state. On the other hand, HC18 monolayer is a liquid-condensed (LC) state at ESP (7 mN m^{-1}). What is clear from the π–A isotherms is that the molecular surface area is very close to a cross-sectional area of the corresponding alkyl chain (~0.18 nm^2). In other words, both HC18 and FCn (n = 16 and 18) molecules at ESP are closely packed with a molecular axis perpendicular to the surface. In spite of this fact, the evaporation rates are not depressed much by the presence of such monolayer at the surface.

The authors measured the surface potential (ΔV) in order to investigate further the reason that can elucidate the present difference between the fluorocarbon and hydrocarbon. The surface potential value was −233 mV for FC10, −146 mV for FC18, +222 mV for HC12, and +374 mV for HC18 at 298.2 K under the respective equilibrium spreading pressure. The above values represent the characteristics of fluorocarbon and hydrocarbon chains; negative values for fluorocarbon and positive values for hydrocarbon [15,29,30]. The small value in magnitude of −146 mV for FC18 indicates that FC18 amount spread at the interface is smaller than FC10 amount, which is consistent with smaller retardation effect of the former and with smaller ESP value. As for HC12 and HC18, on the other hand, the ΔV value for HC18 is higher than that of HC12, which supports better organization of the former molecules at the surface than that of the latter ones. This is also consistent with larger depression effect of HC18 on evaporation rate than that of HC12.

3.4. AFM observation

AFM for the present study provided both topography and phase contrast images. Fig. 9 shows the topography images (200 × 200 nm) of FCn and HCn monolayers transferred to graphite under the equilibrium spreading pressure. All images suggest the monolayer on the water surface to be quite homogeneous. The corresponding phase contrast images (not shown) showed only one homogeneous region. For further examination

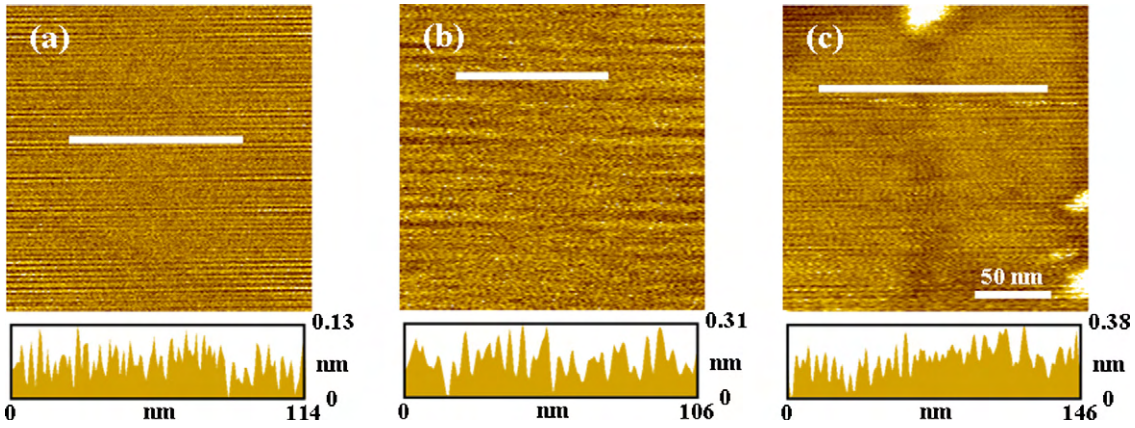

Fig. 9. AFM topography images in a tapping mode at the scan area of 200 × 200 nm: just graphite surface (a) and FC18 (b) and HC18 (c) transferred to graphite at equilibrium spreading pressure. The side profiles indicate cross-section diagrams at respective white line.

on the monolayers, the Brewster angle microscopy (BAM) was applied to the water surface and the surfaces on which FC10 and HC12 monolayers are spread at each equilibrium spreading pressure. The BAM images (not shown) of the above three kinds of surfaces do not show any ordered structure and any difference among them, which is different from an ordered structure of a long alkanol [5]. This observation supports the homogeneous spreading of molecules at the air/water interface, which is consistent with the AFM results. The π–A isotherms, AFM, and BAM images being combined together, the acid molecules are moving around at the surface without forming any ordered structure, which does not lead to much depression of water evaporation rate.

4. Conclusions

Very clear difference between hydrocarbon and fluorocarbon monolayers was made in the water evaporation by the present study, although the evaporation rate does not change much between them. This was made possible by precise examination of the rates using the theory of absolute reaction rate. The evaporation rate of water across an alkanoic acid monolayer decreased with increasing chain length of hydrogenated acids. However, the retardation effect on water evaporation was smaller than that of corresponding 1-alkanol monolayers, and in addition, there was no difference in the activation energy (E_a) or in thermodynamic parameters for an activated complex formation among the alkanoic acids. This is because the small difference in the evaporation rate (k) was not reflected in the activation energy. The E_a value includes mostly the energy to break hydrogen bonds of water molecules. Therefore, the retardation effect of FC*n* or HC*n* monolayer might not be so large as to influence the energy for chemical bond breakage.

On the other hand, the evaporation rate of water across perfluoroalkanoic acid monolayer did not change much with the chain length. It is due to small intermolecular forces among FC*n* hydrophobic chains and to the breakage of more hydrogen bonds of water molecules for FC*n* acids than for HC*n* acids. In addition, water molecules can move more easily through fluorocarbon chains than through hydrocarbon chains. That is, FC*n* molecules would form a monolayer to which water molecules are easy to permeable. The difference in the depression effect on evaporation rate between FC*n* and HC*n* monolayer was supported by their surface potential values, too.

The present basic data for the evaporation rate of water through the insoluble monolayers must be surely valuable for a control of the environment of human beings or the earth using water circulation. In fact, although retardation effect of molecules with a fluorocarbon chain is very small, the small effect is effectively used for cosmetics and other applications.

Acknowledgments

This work was supported by Grant-in-Aid for Scientific Research (B) 17310075 from the Japan Society for the Promotion of Science (JSPS) and by Grant-in-Aid for Exploratory Research 17650139 from the Ministry of Education, Culture, Sports, Science and Technology (MEXT), Japan, and by the Japan–Taiwan Joint Research Program, which are gratefully acknowledged. This work (H.N.) was also supported by Research Fellowships of the Japan Society for the Promotion of Science for Young Scientists (18.9587). And also this work (M.T.) was supported by grants-in-aid for the Kyushu University Foundation, which is greatly appreciated.

Supplementary data

The online version of this article contains additional supplementary data.

Please visit DOI: 10.1016/j.jcis.2007.10.047.

References

[1] R.J. Archer, V.K. LaMer, J. Phys. Chem. 59 (1955) 200–208.
[2] G.T. Barnes, Adv. Colloid Interface Sci. 25 (1986) 89–200.
[3] K.J. Beverley, J.H. Clint, P.D.I. Fletcher, Phys. Chem. Chem. Phys. 1 (1999) 149–153.
[4] Y. Moroi, T. Yamabe, O. Shibata, Y. Abe, Langmuir 16 (2000) 9697–9698.
[5] Y. Moroi, M. Rusdi, I. Kubo, J. Phys. Chem. B 108 (2004) 6351–6358.

[6] M. Rusdi, Y. Moroi, J. Colloid Interface Sci. 272 (2004) 472–479.
[7] M. Rusdi, Y. Moroi, H. Nakahara, O. Shibata, Langmuir 21 (2005) 7308–7310.
[8] J.G. Riess, M.P. Krafft, Chem. Phys. Lipids 75 (1995) 1–14.
[9] J.G. Riess, M.P. Krafft, Biomaterials 19 (1998) 1529–1539.
[10] E. Kissa, Fluorinated Surfactants and Repellents, vol. 97, second ed. (revised and expanded), Marcel Dekker, Basel, NY, 2001.
[11] M.P. Krafft, M. Goldmann, Curr. Opin. Colloid Interface Sci. 8 (2003) 243–250.
[12] M.P. Krafft, J. Polym. Sci. Part A Polym. Chem. 44 (2006) 4251–4258.
[13] K. Ohmori, N. Kudo, K. Katayama, Y. Kawashima, Toxicology 184 (2003) 135–140.
[14] G. Malinverno, I. Colombo, M. Visca, Regul. Toxicol. Pharmacol. 41 (2005) 228–239.
[15] H. Nakahara, S. Nakamura, H. Kawasaki, O. Shibata, Colloids Surf. B 41 (2005) 285–298.
[16] J. Eastoe, A. Rankin, R. Wat, C.D. Bain, D. Styrkas, J. Penfold, Langmuir 19 (2003) 7734–7739.
[17] M. Tsuji, T. Inoue, O. Shibata, Colloids Surf. B, in press; available online 19 July 2007.
[18] G.T. Barnes, J. Hydrol. 145 (1993) 165–173.
[19] G.T. Barnes, Colloids Surf. A 126 (1997) 149–158.
[20] K.J. Beverley, J.H. Clint, P.D.I. Fletcher, Phys. Chem. Chem. Phys. 2 (2000) 4173–4177.
[21] T.W.G. Solomons, Fundamentals of Organic Chemistry, fourth ed., Wiley, New York, 1994.
[22] Y. Moroi, H. Yano, O. Shibata, T. Yonemitsu, Bull. Chem. Soc. Jpn. 74 (2001) 667–672.
[23] M. Rusdi, Y. Moroi, Bull. Chem. Soc. Jpn. 76 (2003) 919–926.
[24] P. Atkins, J. de Paula, Atkins' Physical Chemistry, seventh ed., Oxford Univ. Press, Oxford, 2002.
[25] A. Cary, E.K. Rideal, Proc. R. Soc. London A 109 (1925) 331–338.
[26] E.D. Goddard, J. Colloid Interface Sci. 68 (1979) 196–198.
[27] A.K. Rakshit, G. Zografi, I.M. Jalal, F.D. Gunstone, J. Colloid Interface Sci. 80 (1981) 466–473.
[28] A. Angelova, J. De Coninck, R. Lonov, Supramolecular Sci. 4 (1997) 207–214.
[29] O. Shibata, M.P. Krafft, Langmuir 16 (2000) 10281–10286.
[30] M. Broniatowski, I. Sandez Macho, J. Minones Jr., P. Dynarowicz-Latka, J. Phys. Chem. B 108 (2004) 13403–13411.